

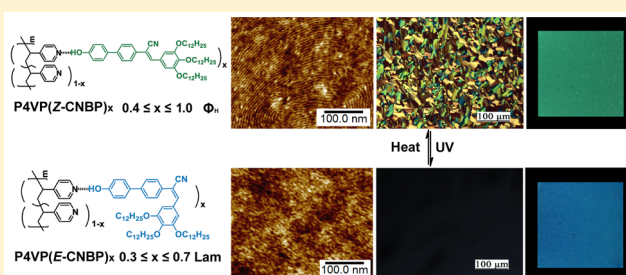
# Supramolecular Fluorescent Polymers Containing $\alpha$ -Cyanostilbene-Based Stereoisomers: *Z/E*-Isomerization Induced Multiple Reversible Switching

Yalan Zhu, Meiqing Zheng, Yuanyang Tu, and Xiao-Fang Chen\*<sup>✉</sup>

State and Local Joint Engineering Laboratory for Novel Functional Polymeric Materials, Jiangsu Key Laboratory of Advanced Functional Polymer Design and Application, College of Chemistry Chemical Engineering and Materials Science, Soochow University, Suzhou 215123, China

## Supporting Information

**ABSTRACT:** Photoresponsive materials play an important role in smart sensors and readable optical devices. The  $\alpha$ -cyanostilbene moiety gathers *Z/E*-isomerization, mesogenic, and aggregation-induced enhanced emission (AIEE) properties together and can be considered as a multifunctional building block bearing luminogen, AIEgen, mesogen, and chromophore characteristics. Here, we report isomerization induced a series of notable reversible switching based on  $\alpha$ -cyanostilbene containing hydrogen-bonded supramolecular polymers. *Z*- and *E*-stereoisomers of dendritic  $\alpha$ -cyanostilbene derivatives (*Z*-CNBP and *E*-CNBP) were hydrogen-bonded with poly(4-vinylpyridine) (P4VP), giving rise to P4VP(*Z*-CNBP)<sub>x</sub> and P4VP(*E*-CNBP)<sub>x</sub>. P4VP(*Z*-CNBP)<sub>x</sub> exhibit a hexagonal columnar ( $\Phi_h$ ) phase at  $0.4 \leq x \leq 1.0$ , while the lamellar phase could be formed for P4VP(*E*-CNBP)<sub>x</sub> at  $0.3 \leq x \leq 0.7$ . P4VP(*Z*-CNBP)<sub>0.8</sub> shows photothermal *E/Z*-isomerization induced reversible switching, including phase structures, surface topographies, birefringence, and fluorescence properties, whereas P4VP(*E*-CNBP)<sub>0.5</sub> exhibits enhanced fluorescence emission upon UV irradiation.



## INTRODUCTION

Stimuli-responsive materials, which adapt to reversibly change their chemical and physical properties in response to an external stimulus, have intensive applications in smart devices, biotechnology, actuators, sensors, etc.<sup>1–5</sup> Toward achieving more complicated functional properties and multiple responsive behaviors in one system in different dimensions and time scale, one of the most used strategies is integrating different functional molecular motives into a system and precisely programming their responsive properties. While with increasing the composition and complicity of system, the challenge to control and manipulate various responses increases dramatically. Single molecular motif exhibiting versatile responsive properties can be considered as the candidate to reduce the complicity of multicomponent integrated functional systems.<sup>6</sup>

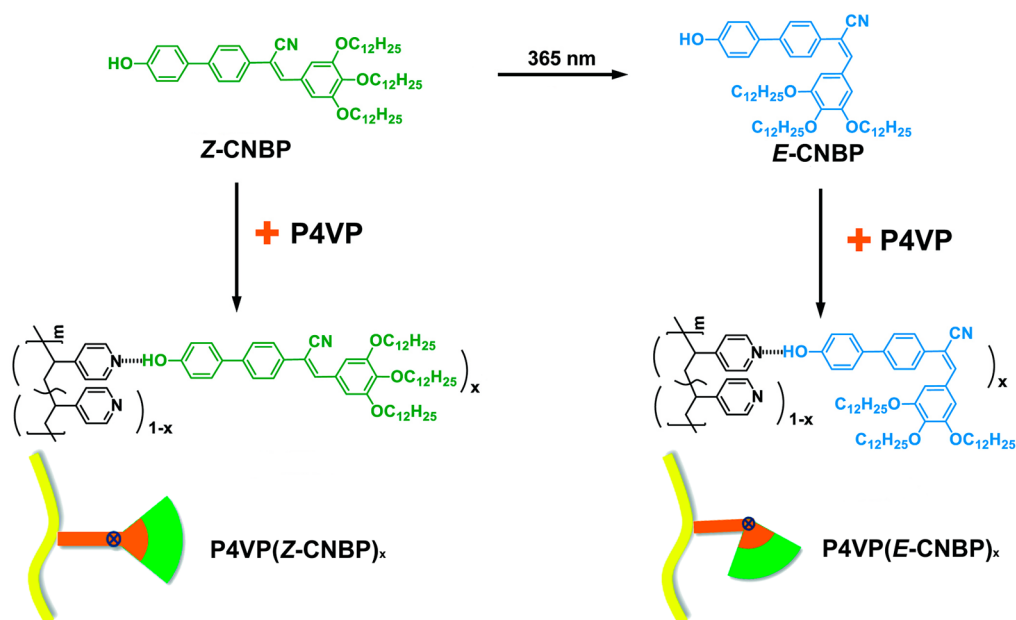
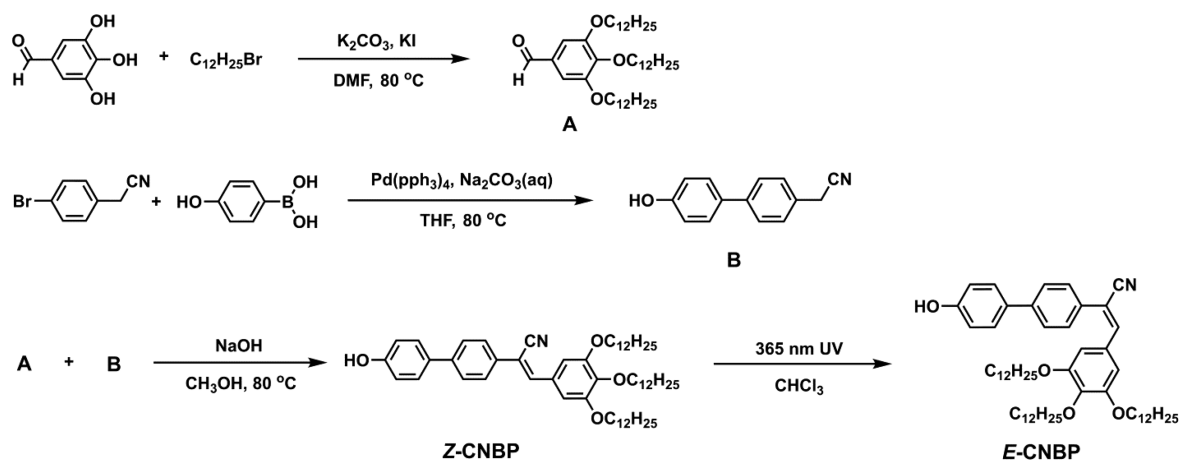
$\alpha$ -Cyanostilbene derivatives,<sup>7–11</sup> which exhibit aggregation-induced enhanced emission (AIEE) properties,<sup>12–14</sup> have received significant attention recently, for their fluorescence can be modulated under various stimuli, exhibiting such as mechanochromic,<sup>15–22</sup> thermochromic,<sup>23–25</sup> and solvatochromic<sup>26,27</sup> responsive properties. Moreover, upon UV irradiation, the  $\alpha$ -cyanostilbene moiety can undergo *Z/E*-isomerization<sup>28–40</sup> that could subsequently induce self-assembly structure changes similar to azobenzene and its derivatives, such as LC-to-iso,<sup>29</sup> gel-to-sol transition,<sup>31</sup> or morphological changes of solution assemblies.<sup>34</sup> Moreover, since the *Z*-isomer generally has a different fluorescence property from the *E*-

isomer, such kind of isomerization could also simultaneously induce fluorescence change. Compared to  $\alpha$ -cyanostilbene, most of photoactive chromophores are nonfluorescent, and additional fluorescent groups should be incorporated to realize isomerization-induced fluorescence switch. As such, it is intriguing to see that  $\alpha$ -cyanostilbene moiety gathers *Z/E*-isomerization, mesogenic, and AIEE properties together and can be considered as an all-round building block bearing luminogen, AIEgen, mesogen, and chromophore characteristics. Although a variety of responsive properties for  $\alpha$ -cyanostilbene derivatives have been explored so far, the reversible switching induced via *E/Z*-isomerization only exists in a limit number of small molecular systems.<sup>28,29,36,37</sup> Concomitant multiple reversible switching in polymeric system is still a challenge.

In recent years, supramolecular side-chain polymers prepared via noncovalent interactions between polymers and molecular additives have been extensively used in construction and fabrication of various hierarchical nanostructures as well as directed assembly of functional molecules within polymer matrix.<sup>41–58</sup> The supramolecular approach offers a facile and efficient route for exploration of novel functional materials with tailored properties, together with solution processability and mechanical properties offered by the polymer chains. Motivated

Received: February 15, 2018

Revised: April 4, 2018

Scheme 1. Synthesis and Schematic Representation of P4VP(*Z*-CNBP)<sub>x</sub> and P4VP(*E*-CNBP)<sub>x</sub>Scheme 2. Synthesis of *Z*-CNBP and *E*-CNBP

by these advantages, we propose to introduce  $\alpha$ -cyanostilbene and its derivatives into supramolecular polymers. The molecular packing of  $\alpha$ -cyanostilbene-based molecules could be modulated via noncovalent interaction, which would further influence their fluorescence and AIEE properties. Meanwhile, the dynamic nature of noncovalent interaction may favor the reversible change about molecular assembly and corresponding physical properties of  $\alpha$ -cyanostilbene derivatives within polymeric system, giving rise to novel multiresponsive functional materials. Last but not least, supramolecular polymers are usually prepared under mild condition via molecular recognition. It gives us an opportunity to precisely incorporate stereoisomers of molecules into supramolecular polymers. For example, the main-chain-type supramolecular polymers based on *Z*- and *E*-isomers of a tetraphenylethene derivative have recently been reported.<sup>59</sup> In our work, both *Z*- and *E*-isomers of  $\alpha$ -cyanostilbene moiety could be complexed with polymer matrix to achieve novel isomer-based supramolecular polymers, which have the identical chemical structure but with different spatial configurations in the side chains. It would help us to gain more insight into the interplay between molecular structures

(especially the molecular configuration) and self-assembled supramolecular structures.

Therefore, in this work, we design a dendritic molecule, CNBP, which contains an  $\alpha$ -cyanostilbene moiety and a phenolic end group as shown in Scheme 1. Its *Z*- and *E*-isomers are named as *Z*-CNBP and *E*-CNBP, respectively. Through hydrogen-bonding interaction, the supramolecular side-chain polymer with poly(4-vinylpyridine) (P4VP) as backbone and CNBP as “side chain” could then be constructed. The configuration effect on self-organized supramolecular structure, as well as the *E/Z*-isomerization induced multi-responsive behavior, was thoroughly investigated. The reversible switching between *Z* and *E* stereoisomers of the  $\alpha$ -cyanostilbene moiety within *Z*-isomer-based supramolecular polymers was successfully realized, which could simultaneously trigger the self-organized structure transformation with concurrent photochromic fluorescence, birefringence, and surface topography switching in this system.

**Table 1. Photophysical Properties and Thermal Behavior of CNBP Isomers**

compounds	$\lambda_{\text{abs}}$ (nm) ( $\epsilon$ ) <sup>a</sup>	$\lambda_{\text{em}}$ (nm) ( $\Phi_f$ ) <sup>b</sup>	$\lambda_{\text{em}}$ (nm) ( $\Phi_s$ ) <sup>c</sup>	phase transition $T$ (°C) <sup>d</sup>
Z-CNBP	362 (21000)	445 (0.005)	499 (0.28)	Cr 50 Sm 78 Iso
E-CNBP	336 (10700)	416 (0.003)	481 (0.03)	Cr <sup>1</sup> 55 Cr <sup>2</sup> 75 Iso

<sup>a</sup>Absorption maximum wavelength (molar extinction coefficient) of CNBP in chloroform ( $1 \times 10^{-4}$  mol/L). <sup>b</sup>Emission maximum wavelength (quantum yields obtained from absolute measurements in an integrating sphere) of CNBP in chloroform ( $2 \times 10^{-5}$  mol/L) solution. <sup>c</sup>Emission maximum wavelength (quantum yields) of CNBP in solid state. <sup>d</sup>Data determined by DSC, temperatures at the maximum of the phase transition peaks in the second heating cycle at a scanning rate of 10 °C/min. Cr: crystalline phase; Sm: smectic phase; Iso: isotropic liquid.

## RESULTS AND DISCUSSION

**Synthesis and Characterization of CNBP and Corresponding Supramolecular Polymers.** As shown in Scheme 2, Z-CNBP was first synthesized and purified. By irradiating Z-CNBP solution under 365 nm UV irradiation, Z- to E-isomerization was triggered instantly as detected via UV-vis absorption (Figure S1) and <sup>1</sup>HNMR spectra (Figure S2). After 2 h, the CDCl<sub>3</sub> solution of Z-CNBP (10 mg/mL) in an NMR tube reached their photostationary state with the molar ratio of E- and Z-CNBP as 4:1. So E-CNBP was prepared via UV irradiating Z-CNBP in CHCl<sub>3</sub> solution for at least 2 h and then separated and purified via column chromatography. As we expected, due to their different molecular configurations, Z-CNBP and E-CNBP have distinct photophysical properties and thermal behavior as listed in Table 1. Z-CNBP shows fluorescent liquid crystalline behavior with the AIEE effect while E-CNBP does not (Figures S3–S7). Both Z- and E-isomers were hydrogen-bonded with P4VP to form P4VP(Z-CNBP)<sub>x</sub> and P4VP(E-CNBP)<sub>x</sub> complexes, respectively, via the solution blending method. The *x* here refers to the molar ratio of CNBP to 4VP repeating unit. The formation of hydrogen bond in polymer complexes can be confirmed via FT-IR spectra as shown in Figure 1. The absorption bands of pyridine ring in pure P4VP appear at 1597, 1415, and 993 nm<sup>-1</sup>. For P4VP(Z-CNBP)<sub>x</sub> complexes in Figure 1a, the absorption bands at 1597 and 1415 nm<sup>-1</sup> gradually shift to 1604 and 1421 nm<sup>-1</sup>, respectively. This result is consistent with the previously reported hydrogen-bonded supramolecular polymers containing P4VP and molecular additives with phenolic end groups.<sup>40,48,52,55,56</sup> The absorption band at 993 nm<sup>-1</sup> tends to shift to 1008 nm<sup>-1</sup>, which overlaps with the absorption peaks from Z-CNBP in this case. The hydrogen bond formation in P4VP(E-CNBP)<sub>x</sub> complexes can also be confirmed according to the similar absorption band shifts of pyridine ring as shown in Figure 1b. <sup>1</sup>HNMR spectra of polymer complexes confirm that Z- and E-isomers are quite stable in polymer complexes during complexation (Figure S8) and thermal annealing below 90 °C (Figure S9).

**Phase Behavior of Isomer-Based Supramolecular Polymer.** After complexation, the self-organized structures of obtained polymer complexes and their thermal behaviors were studied via small-angle X-ray scattering (SAXS) and differential scanning calorimetry (DSC). As shown in Figure 2a, the SAXS profiles of P4VP(Z-CNBP)<sub>x</sub> show characteristic *x*-dependent phase behavior (Figure 2a). When  $x \leq 0.3$ , only a weak and broad scattering peak in the low angle region is detected, corresponding to amorphous state. When  $x \geq 0.4$ , the SAXS profiles show three peaks at  $q^*$ ,  $\sqrt{3}q^*$ , and  $2q^*$  respectively corresponding to (10), (11), and (20) reflections. This suggests clearly the formation of hexagonal columnar ( $\Phi_h$ ) structure. The lattice parameter *a* of  $\Phi_h$  structure, which is associated with the diameter of each cylinder, reduces gradually from 6.66 nm at  $x = 0.4$  to 5.92 nm at  $x = 1.0$ . Reminding the calculated

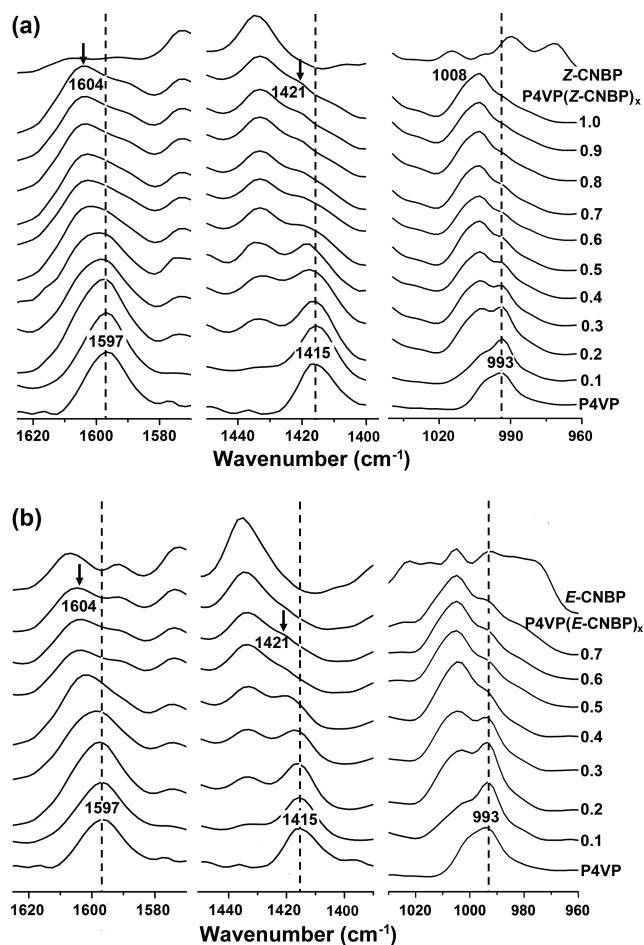


**Figure 1.** FT-IR spectra of pure P4VP, Z-CNBP, E-CNBP, and P4VP complexes containing (a) Z-CNBP and (b) E-CNBP of the different molar ratios (*x*) to the pyridine units.

molecular length in the most extended form is 3.2 nm for Z-CNBP with all-trans conformation of the alkoxy chains, the schematic inset in Figure 2a illustrates that the hydrogen-bonded dendritic Z-CNBP molecules are wrapping around the P4VP chains, giving rise to cylindrical assemblies. The supramolecular cylinders are parallel to each other, forming a hexagonal packing.<sup>45–56</sup> Upon increasing the content of Z-CNBP, the polymer backbones within the cylinder become more stretched to accept more grafted Z-CNBP molecules, which finally shrink the lateral size of each cylinder. Z-CNBP itself possesses lamellar structure in liquid crystalline phase as shown in Figure S7 and tends to crystallize when cooling to room temperature. After being hydrogen-bonded with P4VP, the  $\Phi_h$  structure appears at  $0.4 \leq x \leq 1.0$ , and no phase separation is detected via SAXS and DSC, indicating the formation of homogeneous complex with highly ordered supramolecular structure.

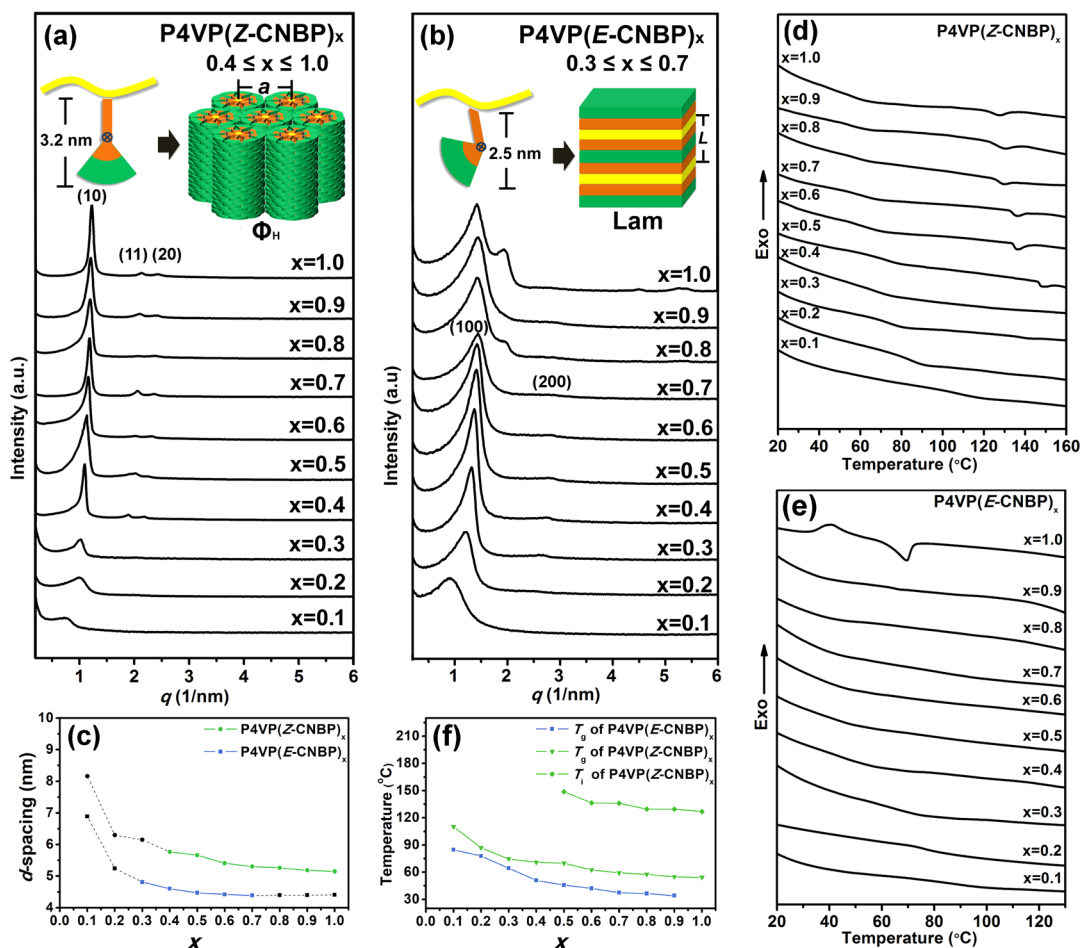


**Figure 2.** SAXS profiles of P4VP(Z-CNBP)<sub>x</sub> (a) and P4VP(E-CNBP)<sub>x</sub> (b) at room temperature. (c) The *d*-spacing of the first scattering peak as a function of *x*. DSC curves of P4VP(Z-CNBP)<sub>x</sub> (d) and P4VP(E-CNBP)<sub>x</sub> (e) during the second heating cycle at the rate of 10 °C/min under a N<sub>2</sub> atmosphere. (f) *T*<sub>g</sub> and *T*<sub>i</sub> of P4VP(Z-CNBP)<sub>x</sub> and P4VP(E-CNBP)<sub>x</sub> as a function of *x*.

When the complexed CNBP adopts *E* configuration, the resulting P4VP(*E*-CNBP)<sub>x</sub> samples possess different self-organized structures as shown in Figure 2b. Only two scattering peaks with a *q*-ratio of 1:2 are observed at 0.3 ≤ *x* ≤ 0.7, indicating the existence of lamellar structure as shown in the schematic inset in Figure 2b. The layer thickness (*L*) slightly decreases from 4.7 to 4.3 nm as increasing *x*. When further increasing the content of *E*-CNBP, additional scattering peaks could be detected, which is due to the crystalline *E*-CNBP that is macroscopically separated from P4VP(*E*-CNBP)<sub>x</sub>. The plots of the *d*-spacing of the first scattering peak as a function of *x* in Figure 2c clearly show that P4VP(Z-CNBP)<sub>x</sub> have relatively larger *d*-spacing than that of P4VP(*E*-CNBP)<sub>x</sub> due to the different molecular size between *Z*- and *E*-isomers.

It is clearly to see that the molecular configuration dramatically influences the self-organized structures. In our work, the *Z*-CNBP molecule possesses hemipharmidic structure that is the combination of rod-like segment and Percec-type dendron. It is well-known that Percec-type dendrons are frequently used to realize the columnar phase formation, while in this case the rod-like segment here also plays an important role to stabilize the columnar structure. It can be found from the published data that the minimum content of dendritic side chains to form Φ<sub>h</sub> phase structure decreases from *x* = 0.7 to *x* = 0.3 with increasing the length of rigid part in hydrogen-bonded supramolecular dendronized

polymers.<sup>51–56</sup> In our work, *Z*- and *E*-CNBP have the same dendron but the different configurations in rigid part. Based on SAXS results, the bent-shaped *E*-isomer could not favor the columnar packing. The lamellar structure appearance is attributed to the microphase separation between aromatic polar and aliphatic nonpolar part in polymer complexes. Meanwhile, the bulky shape of *E*-isomer hinders the hydrogen-bonding interaction to some extent. Only when *x* < 0.8 could homogeneous complexes be prepared.

The isomer-based supramolecular polymers also show different thermal behavior as revealed by DSC. As shown in Figure 2d, the glass transition temperature (*T*<sub>g</sub>) of P4VP(Z-CNBP)<sub>x</sub> decreases from 110 °C at *x* = 0.1 to 58 °C at *x* = 1.0. When *x* ≥ 0.5, an endothermic peak originating from Φ<sub>h</sub> to isotropic phase transition (*T*<sub>i</sub>) becomes detectable, and the *T*<sub>i</sub> gradually decreases from 148 °C at *x* = 0.5 to 128 °C at *x* = 1.0. While for P4VP(*E*-CNBP)<sub>x</sub>, only *T*<sub>g</sub> is detected as shown in Figure 2e, which is also decreased with increasing the content of *E*-CNBP. No phase transition could be observed when *x* < 1.0. Until *x* = 1.0, macrophase separation could be detected in Figure 2e. The decline of *T*<sub>g</sub> with increasing *x* is due to the plasticization effect of molecules. Meanwhile, the *T*<sub>g</sub> of P4VP(*E*-CNBP)<sub>x</sub> is also lower than that of P4VP(Z-CNBP)<sub>x</sub> as shown in Figure 2f, indicating *E*-CNBP has larger plasticization effect than *Z*-CNBP. It is attributed to the different configurations of *E*/*Z*-stereoisomers. The rigid

conjugated segment offers *Z*-CNBP stronger intermolecular interaction than *E*-CNBP, which finally influenced the  $T_g$  of corresponding polymer complexes.

The *E/Z*-stereoisomer-based supramolecular polymers show distinctly different self-assembly behavior, including complexation ability, phases transition, and phase structure. It is the first time to directly study the effect of molecular configuration on the self-organized structures in supramolecular polymers. After complexation, homogeneous polymer complexes could be obtained, which could be processed into fibers, films, or other forms. A more intriguing thing is the photoresponsive property of CNBP still exists in a supramolecular system. The isomerization-induced physical properties switching in polymer complexes were thus systematically studied.

***E/Z*-Isomerization Induced Multiple Reversible Switching.** Figure 3a shows polarized optical microscopy

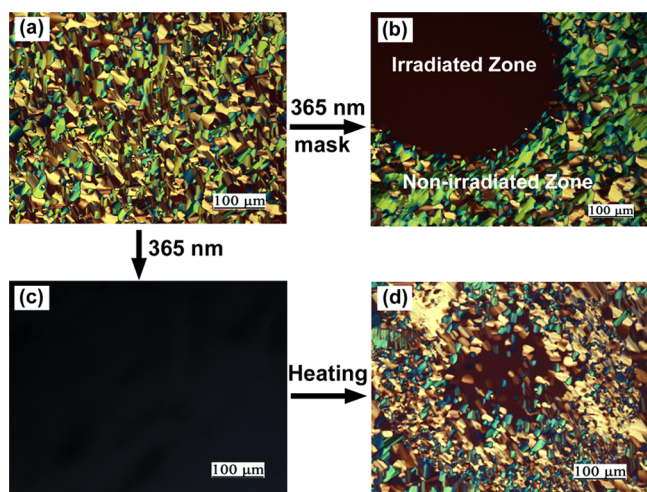


**Figure 3.** POM photographs of P4VP(Z-CNBP)<sub>0.8</sub> film taken at 125 °C (a) and then UV irradiated for 10 min through a mask (b). (c) POM photograph of fully irradiated film. (d) The irradiated film is heated to isotropic state at 140 °C and then cooled to 125 °C.

(POM) pictures of P4VP(Z-CNBP)<sub>0.8</sub> taken at 125 °C. Characteristic fan-like textures from columnar phase were obtained by slowly cooling P4VP(Z-CNBP)<sub>0.8</sub> from the isotropic state. Upon UV irradiation through a mask for 10 min, the birefringence of irradiated zone decreases dramatically, whereas other region still keeps its textures (Figure 3b). By heating the fully irradiated film (Figure 3c) to its isotropic state at 140 °C for 10 min and then slowly cooling down to 125 °C, characteristic fan-like LC texture appears again (Figure 3d). The distinct birefringence contrast is associated with the phase structure change upon UV irradiation. SAXS experiments directly revealed the structure evolution of P4VP(Z-CNBP)<sub>0.8</sub> before and after UV irradiation. As shown in Figure 4a, the as-prepared P4VP(Z-CNBP)<sub>0.8</sub> sample exhibits  $\Phi_h$  structure with a parameter of 6.09 nm. After UV irradiation, the intensities of scattering peaks decrease and become broad, together with the disappearing of (11) scattering peak, indicating the phase structure transforms to lamellar structure ( $L = 5.11$  nm). Meanwhile,  $q$  value of the first (10) peak increased from 1.19 to 1.23 nm<sup>-1</sup>. Then, after thermal treatment, the corresponding SAXS profile confirms the formation of  $\Phi_h$  structure with a parameter of 6.05 nm, which is similar to the initial state (Figure 4a). It is clearly demonstrated a reversible responsive behavior. <sup>1</sup>H NMR measurement confirms that the reversible

structure change is attributed to the *E/Z*-isomerization of CNBP (Figure S10). Upon UV irradiation, around 37% *E*-CNBP appeared in polymer complex. Then, after subsequent heating process, most of *E*-CNBP molecules convert to *Z*-CNBP, and the content of *E*-CNBP decreased to 5%. It should be noted that in some reported cases cyanostilbene can also take [2 + 2] cycloaddition in the bulk phase.<sup>60–62</sup> It could be identified as the appearance of a singlet at 5.39 ppm in <sup>1</sup>H NMR, which is due to the cyano-substituted cyclobutane ring. In the polymer complexes systems, only *Z*- and *E*-isomers are detected and no other reactions take place during UV irradiation and thermal treatment (Figure S10). So it is the photothermal isomerization that induced the reversible phase transition in the film. Meanwhile, the appearance of *E*-CNBP during UV irradiation disturbed the columnar structure formation.

The self-organized ordered structure and orientation of P4VP(Z-CNBP)<sub>0.8</sub> in thin film could also be detected via atomic force microscopy (AFM) and grazing-incidence SAXS (GISAXS). A thin film of P4VP(Z-CNBP)<sub>0.8</sub> with the thickness around 90 nm was prepared via spin-coating of its chloroform solution (10 mg/mL) and subsequent thermal annealing for 12 h at 80 °C. The GISAXS pattern of annealed film in Figure 4b confirms the  $\Phi_h$  structure with parallel orientation in the film. Meanwhile, the corresponding AFM height and phase images in Figure 4c clearly show fingerprint-like morphology on the surface, which is a characteristic topography associated with the parallel alignment of cylinders in the thin film as confirmed via GISAXS. Since the surface topography of the film is related to the self-organized structure, the photoinduced structure change would further induce the surface topographical change in the film. After UV irradiation for 10 min, the fingerprint pattern disappears, instead of irregular morphology as shown in Figure 4c. Meanwhile, the diffraction pattern from  $\Phi_h$  structure also disappears in GISAXS, instead of diffused and weak halo from lamellar structure. Correspondingly, the static contact angle of a water droplet ( $\theta_w$ ) on the P4VP(Z-CNBP)<sub>0.8</sub> film decreased from 104° to 100° after UV irradiation, since the exposure of the hydrophobic alkyl tail of CNBP unit to the topmost surface changed because of the *E/Z*-isomerization. By heating up to 140 °C and then slowly cooling to its LC state, both hexagonal diffraction pattern in GISAXS (Figure 4b) and the fingerprint topographical pattern in AFM (Figure 4c) appear again.

After knowing the relationship between molecular configuration and self-organized structures, the stimuli-responsive fluorescent properties of P4VP(Z-CNBP)<sub>x</sub> are readily to be revealed. Figure 5a shows the photoluminescence (PL) spectra of P4VP(Z-CNBP)<sub>0.8</sub> film upon UV irradiation at different times. The emission peak of initial state is at 493 nm. During UV irradiation at room temperature, the intensity of emission peak increases gradually and becomes constant after 90 min. Meanwhile, the peak position shifts to 471 nm. The hypsochromic shift of the emission peak means the conjugated length decreases after irradiation, when *Z*-CNBP converts to *E*-CNBP. As a comparison, fluorescence change of pure *Z*-CNBP via UV irradiation stimuli at room temperature is presented in the inset to Figure 5a. During UV irradiation the intensity and peak position did not change much even after 2 h, which is due to the crystalline structure that prevents the isomerization from *Z*- to *E*-isomers. Different from pure *Z*-CNBP, the complexed *Z*-CNBP in polymer matrix is well-dispersed with the aid of hydrogen-bonding interaction. No crystalline structure formed at room temperature based on SAXS, DSC, and POM studies.

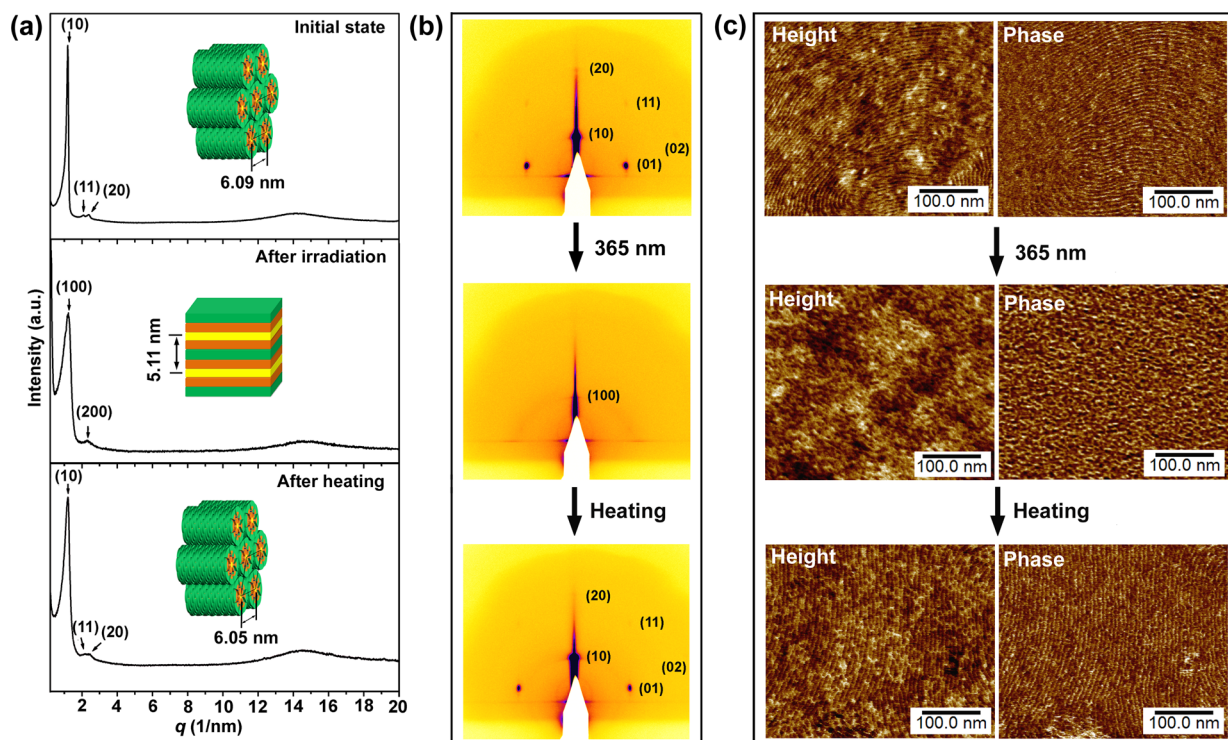


**Figure 4.** (a) SAXS profiles of P4VP(Z-CNBP)<sub>0.8</sub> recorded at initial state, after irradiation and after heating. GISAXS patterns (b) and AFM height and phase images (c) of P4VP(Z-CNBP)<sub>0.8</sub> thin film upon UV irradiation and thermal treatment.

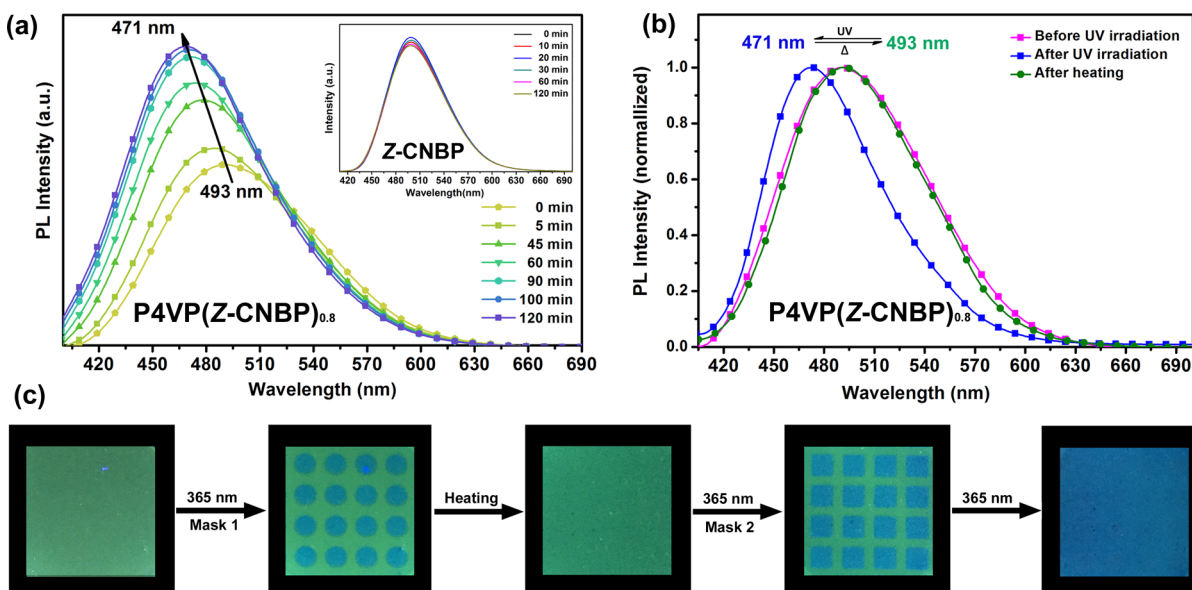


**Figure 5.** (a) Photoluminescence (PL) spectra of P4VP(Z-CNBP)<sub>0.8</sub> film upon UV irradiation for different times at room temperature. Inset: PL spectra of Z-CNBP film upon UV irradiation for different times at room temperature. (b) PL spectra of P4VP(Z-CNBP)<sub>0.8</sub> film before (pink squares) and after (blue squares) UV irradiation and subsequent thermal treatment (green circles). (c) Fluorescence images of P4VP(Z-CNBP)<sub>0.8</sub> film during UV irradiation and thermal treatment processes, taken under 365 nm UV light. Both the diameter of each circular hole and the side length of each square hole are 2 mm.

The  $T_g$  of P4VP(Z-CNBP)<sub>0.8</sub> is 58 °C, which is above the room temperature, so the *E/Z*-isomerization induced fluorescence change could take place even below the  $T_g$ . A more exciting thing is after heating the irradiated film at 140 °C for 10 min, the emission peak returns to 493 nm, which is the same as the initial state as shown in Figure 5b. The reversible fluorescence switching is also realized in the polymer complex.

Since the PL intensity and wavelength are quite different before and after UV irradiation, fluorescence patterns with dual emission colors would be easily obtained by UV irradiating P4VP(Z-CNBP)<sub>0.8</sub> film through a mask. Figure 5c depicts the fluorescence images of P4VP(Z-CNBP)<sub>0.8</sub> film during the writing–erasing cycles. The pristine film exhibits green fluorescence under UV light. After UV irradiation for 60 min, the irradiated zone became blue. It is worthwhile to point out

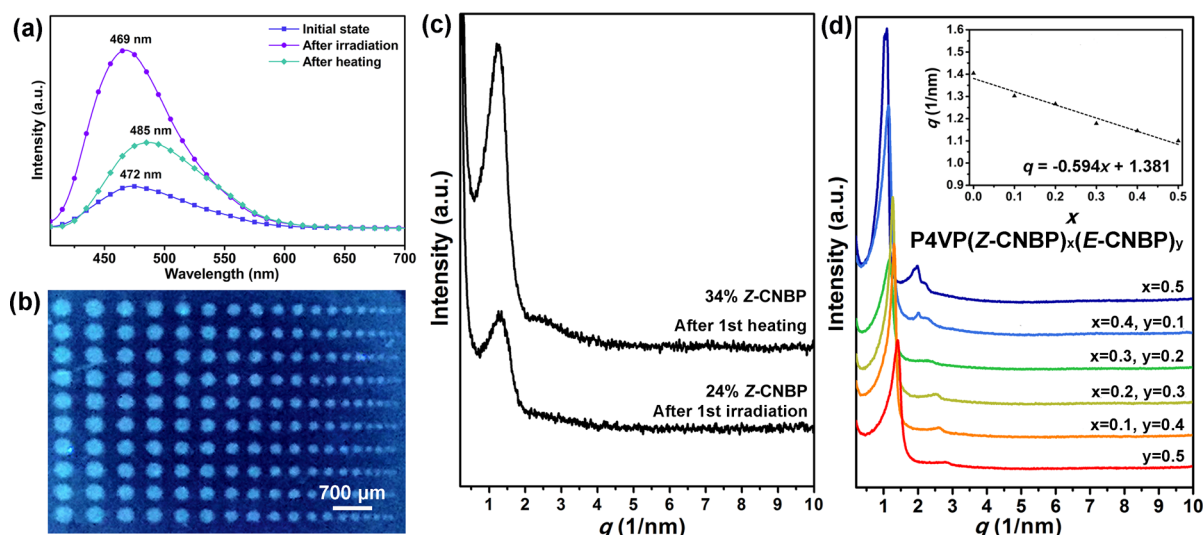


**Figure 6.** (a) PL spectra of P4VP(*E*-CNBP)<sub>0.5</sub> film before (blue squares) and after (purple circles) UV irradiation and subsequent thermal treatment (green rhombuses). (b) Fluorescence image of irradiated P4VP(*E*-CNBP)<sub>0.5</sub> film after UV through mask taken under 365 nm UV irradiation. (c) SAXS profiles of P4VP(*E*-CNBP)<sub>0.5</sub> after first UV irradiation and subsequent first heating treatment. (d) SAXS profiles of P4VP(*Z*-CNBP)<sub>*x*</sub>(*E*-CNBP)<sub>*y*</sub> (*x* + *y* = 0.5). Inset: *q* as a function of *x* for P4VP(*Z*-CNBP)<sub>*x*</sub>(*E*-CNBP)<sub>*y*</sub>, with *x* + *y* = 0.5.

that fluorescence change is more sensitive than other switching behaviors. The dual color pattern could be identified by naked eyes only after 1 min. The best contrast pattern could be obtained after 60 min. Then, the fluorescence pattern could be erased, and the whole film appears green fluorescence again by heating to 140 °C for 10 min. The reversible switching is repeatable. Different fluorescence patterns could be written again in the same film by using different masks as shown in Figure 5c. As a comparison, we also dispersed *Z*-CNBP into polystyrene (PS) matrix with the same molar ratio (*n*<sub>*Z*-CNBP</sub>:*n*<sub>St</sub> = 0.8:1) and with the same preparation condition. In this case, *Z*-CNBP is dispersed into PS without hydrogen-bonding interaction. However, only the PL intensity decreased during UV irradiation (Figure S11). Meanwhile, the light-induced PL change is irreversible. It is hard to return to its initial state by heating to 140 °C or even higher temperatures (Figure S12). So the fluorescence pattern written into the *Z*-CNBP/PS film is not erasable, and the film even becomes heterogeneous during heating/irradiation cycles (Figure S13). Comparing to *Z*-CNBP/PS film, the hydrogen-bonded P4VP(*Z*-CNBP)<sub>*x*</sub> film is quite uniform and stable during UV irradiation and thermal treatment. At the same time, the hydrogen-bonding interaction could keep ordered arrangement of CNBP molecules within the polymer matrix. The fluorescent property of polymer complex is associated with both molecular structure and supramolecular self-organized structure, exhibiting a typical reversible responsive characteristic.

Contrary to P4VP(*Z*-CNBP)<sub>*x*</sub> complex, the corresponding P4VP(*E*-CNBP)<sub>*x*</sub> show irreversible responsive behavior. On the basis of UV–vis spectra (Figure S1) results, in pure *E*-CNBP state, only a small amount of *E*-CNBP could convert to *Z*-CNBP under UV irradiation according to *E*/*Z*-isomerization equilibrium. The interesting thing is the appearance of *Z*-CNBP could “turn on” the fluorescence in polymer complexes. For example, the as-prepared film of P4VP(*E*-CNBP)<sub>0.5</sub> shows PL emission peak at 472 nm as shown in Figure 6a. After irradiation upon 365 nm UV light at room temperature, the PL intensity increases dramatically and then reaches a constant at 469 nm after 1 h. The high contrast fluorescence pattern was

easily obtained by UV irradiating P4VP(*E*-CNBP)<sub>0.5</sub> film through a mask. The irradiated zone shows enhancement of fluorescence, as shown in Figure 6b. Then, by heating at 140 °C, the intensity of PL peak decreases, and the peak position red-shifts to 485 nm. <sup>1</sup>H NMR detected the content of *Z*-CNBP was 22% after first UV irradiation and 35% after first heating (Figure S14), indicating an irreversible switching.

SAXS also shows that the intensity of scattering peaks decreases significantly after irradiation. Then by thermal treatment, the intensity of scattering peak increases (Figure 6c). The scattering vector *q* of the first peak at low angle region is 1.31 nm<sup>−1</sup> (after irradiation) and 1.28 nm<sup>−1</sup> (after heating). The relationship between *q* and the content of isomers could be obtained by complexing both *E*-CNBP and *Z*-CNBP with P4VP, and the SAXS profiles of P4VP(*Z*-CNBP)<sub>*x*</sub>(*E*-CNBP)<sub>*y*</sub> (*x* + *y* = 0.5) are presented in Figure 6d. When *x* ≥ 0.4, Φ<sub>h</sub> structure appears, below which only the lamellar structure exists. The plot of *q* vs *x* is shown in the inset of Figure 6d as a linear fit of the experimental data with *q* = −0.594*x* + 1.381. Thus, the content of *Z*-CNBP in the polymer complex could be estimated via a *q*–*x* plot, which is 24% (after irradiation) and 34% (after heating). The result is also close to that obtained from <sup>1</sup>H NMR results.

## CONCLUSION

In summary, we have successfully incorporated *Z*- and *E*-stereoisomers of *α*-cyanostilbene derivatives into supramolecular polymers via hydrogen-bonding interaction in an effective and facile way. The corresponding P4VP(*Z*-CNBP)<sub>*x*</sub> and P4VP(*E*-CNBP)<sub>*x*</sub> complexes have different self-assembly behavior and stimuli-responsive properties. P4VP(*Z*-CNBP)<sub>*x*</sub> possess Φ<sub>h</sub> structure at 0.4 ≤ *x* ≤ 1.0, while lamellar structure could be formed for P4VP(*E*-CNBP)<sub>*x*</sub> at 0.3 ≤ *x* ≤ 0.7. The P4VP(*Z*-CNBP)<sub>0.8</sub> film exhibited photothermal *E*/*Z*-isomerization induced concomitant multiple reversible switching, including the self-organized structures, surface topographies and properties, birefringence, and fluorescence intensity and color. The P4VP(*E*-CNBP)<sub>0.5</sub> film shows irreversible switching and enhanced fluorescence emission upon UV irradiation.

Thus, by controlling over the molecular configuration in supramolecular polymer system, we can precisely tune the phase structure and functional responsive properties at the same time. On the basis of those results, it would be intriguing to further incorporate various functional moieties into cyanostilbene-based supramolecular system to develop new kind of smart photoactive materials.

## EXPERIMENTAL SECTION

**Materials.** Z-CNBP was synthesized according to the synthetic route as shown in Scheme 2 and purified through column chromatography. E-CNBP was obtained by irradiating concentrated solution of Z-CNBP in CHCl<sub>3</sub> by 365 nm UV light for at least 2 h to get a mixture of Z-CNBP and E-CNBP. E-CNBP was then separated and purified by column chromatography. Poly(4-vinylpyridine) (P4VP, weight-average molecular weight,  $M_w = 6.0 \times 10^4$ , PDI = 1.3) was purchased from Polymer Source Inc. Other materials were used as received. The detailed information is listed in the Supporting Information.

**Synthesis of 3,4,5-Tris(dodecyloxy)benzaldehyde (Compound A).** K<sub>2</sub>CO<sub>3</sub> (2.81 g, 20.33 mmol) and KI (catalytic amount) were added to a solution of 3,4,5-trihydroxybenzaldehyde monohydrate (1.00 g, 5.81 mmol) in dry DMF (20 mL). The mixture was stirred at 80 °C. 1-Bromododecane (5.62 mL, 23.24 mmol) was slowly dropped into the mixture. The reaction lasted overnight. After cooling to RT, the mixture was poured into brine and extracted with dichloromethane. The organic layer was dried by anhydrous magnesium sulfate, and the solvent was evaporated by a rotor vapor. The product (3.26 g, 85%) was obtained by column chromatography using ethyl acetate and *n*-hexane (1:10 v/v). <sup>1</sup>H NMR (CDCl<sub>3</sub>) δ [ppm]: 9.83 (s, 1H, -CHO), 7.08 (s, 2H, Ar-H), 4.04 (m, 6H, -OCH<sub>2</sub>), 1.79 (m, 6H, -CH<sub>2</sub>), 1.48 (m, 6H, -CH<sub>2</sub>), 1.26 (m, 48H, -CH<sub>2</sub>), 0.88 (t, 9H, -CH<sub>3</sub>).

**Synthesis of (4'-Hydroxybiphenyl-4-yl)acetonitrile (Compound B).** 4-Bromophenylacetonitrile (1.7 g, 8.6 mmol) and 4-hydroxybenzeneboronic acid (1.2 g, 8.7 mmol) were dissolved in 60 mL of THF. Then, 30 mL of an aqueous sodium carbonate (6.4 g, 60 mmol) solution was added. Under a nitrogen atmosphere, Pd(PPh<sub>3</sub>)<sub>4</sub> (0.1 g, 0.08 mmol) was added, and the solution was refluxed for 12 h. After cooling to room temperature, the mixture was neutralized by hydrochloric acid and then extracted with brine/ethyl acetate for three times. The collected organic phase was dried by anhydrous magnesium sulfate. The crude product was purified by column chromatography using petroleum ether and ethyl acetate (2:1 v/v) to obtain a white solid. Yield: 1.08 g, 60%. <sup>1</sup>H NMR (CDCl<sub>3</sub>) δ [ppm]: 9.58 (s, 1H, -OH), 7.54 (d, 2H, Ar-H), 7.46 (d, 2H, Ar-H), 7.36 (d, 2H, Ar-H), 6.90 (d, 2H, Ar-H), 3.78 (s, 2H, -CH<sub>2</sub>).

**Synthesis of Z-2-(4'-Hydroxybiphenyl-4-yl)-3-(3,4,5-tris(dodecyloxy)phenyl)acrylonitrile (Z-CNBP).** Compound A (540 mg, 0.82 mmol), compound B (171.6 mg, 0.82 mmol), and sodium hydroxide (200 mg, 5 mmol) in 10 mL of anhydrous methanol were stirred under a nitrogen atmosphere at 50 °C for 12 h. After cooling to room temperature, the mixture was neutralized by hydrochloric acid. The yellow precipitation was collected by filtration and extracted with water and ethyl acetate. Yield: 0.507g, 80%. <sup>1</sup>H NMR (CDCl<sub>3</sub>) δ [ppm]: 7.76 (d, 2H, Ar-H), 7.67 (d, 2H, Ar-H), 7.57 (d, 2H, Ar-H), 7.50 (s, 1H, -CH-), 7.21 (s, 2H, Ar-H), 6.98 (d, 2H, Ar-H) 4.10 (m, 6H, -OCH<sub>2</sub>-), 1.73–1.87 (m, 6H, -OCH<sub>2</sub>CH<sub>2</sub>-), 1.26–1.54 (m, 54H, -(CH<sub>2</sub>)<sub>9</sub>-), 0.88 (t, 9H, -CH<sub>3</sub>). MS: calcd for C<sub>57</sub>H<sub>87</sub>NO<sub>4</sub>, 849.7 Da; found *m/z* 850.7 [M + H]<sup>+</sup>.

**Synthesis of (E)-2-(4'-Hydroxybiphenyl-4-yl)-3-(3,4,5-tris(dodecyloxy)phenyl)acrylonitrile (E-CNBP).** A concentrated solution of Z-CNBP in CHCl<sub>3</sub> was irradiated under 365 nm UV light for 3 h to get a mixture of Z-CNBP and E-CNBP. E-CNBP was separated from the mixture and purified by column chromatography as a powder in 69% yield. <sup>1</sup>H NMR (CDCl<sub>3</sub>) δ [ppm]: 7.55 (d, 2H, Ar-H), 7.45 (m, 4H, Ar-H), 7.23 (s, 1H, -CH), 6.90 (d, 2H, Ar-H), 6.28 (s, 2H, Ar-H), 4.92 (s, 1H, -OH), 3.94 (t, 2H, -OCH<sub>2</sub>-), 3.65 (t, 4H, -OCH<sub>2</sub>-), 1.73–1.87 (m, 6H, -OCH<sub>2</sub>CH<sub>2</sub>-), 1.26–1.54 (m, 54H,

-(CH<sub>2</sub>)<sub>9</sub>-), 0.88 (t, 9H, -CH<sub>3</sub>). MS: calcd for C<sub>57</sub>H<sub>87</sub>NO<sub>4</sub>, 849.7 Da; found *m/z* 850.7 [M + H]<sup>+</sup>.

**Polymer Complex Preparation.** The supramolecular complexes were prepared as the following procedure. P4VP and CNBP (Z- or E-isomers) were separately dissolved into chloroform to get 5 wt % solutions. In order to obtain the P4VP(CNBP)<sub>x</sub> complex, P4VP and CNBP solutions were mixed together with calculated proportion related to *x*. A homogeneous solution was obtained. After mechanical stirring for 24 h at room temperature, the solvent was slowly evaporated. The product was then placed in a vacuum oven at 35 °C to remove residual solvent. The supramolecular complex was thus obtained.

**Thin Film Preparation.** P4VP and CNBP were separately dissolved in chloroform to yield 10 mg/mL solutions and then mixed in proportion to give homogeneous solutions. The solution was filtered with 0.2 μm PTFE filters and spin-coated onto a freshly cleaned silicon wafer at the rotating speed of 2000 rpm for 30 s to get the film around 80–90 nm as judged from spectroscopic ellipsometer.

**Isomerization Experiment.** Photoinduced isomerization was performed under UV irradiation from a hand-held UV light (1.0 mW/cm<sup>2</sup>) at a distance of 5 cm. Solutions for UV-vis tests were irradiated in quartz cells at room temperature. Solutions for NMR experiments were irradiated in NMR tube at room temperature. Films were irradiated at the mesophase (125 °C) or at room temperature as required.

## ASSOCIATED CONTENT

### Supporting Information

The Supporting Information is available free of charge on the ACS Publications website at DOI: 10.1021/acs.macromol.8b00347.

Materials, instruments, and measurements; Figure S1 (UV-vis spectra of CNBP); Figure S2 (<sup>1</sup>H NMR of CNBP); Figure S3 (POM of CNBP); Figure S4 (PL spectra of CNBP); Figure S5 (PL spectra of Z-CNBP-AIEE effect); Figure S6 (DSC of CNBP); Figure S7 (XRD of CNBP); Figure S8 (<sup>1</sup>H NMR of P4VP(Z-CNBP)<sub>x</sub>); Figure S9 (<sup>1</sup>H NMR of P4VP(Z-CNBP)<sub>0.8</sub> and P4VP(E-CNBP)<sub>0.5</sub>); Figure S10 (<sup>1</sup>H NMR of P4VP(Z-CNBP)<sub>0.8</sub>); Figures S11 and S12 (PL spectra of PS/Z-CNBP); Figure S13 (fluorescence images of PS/Z-CNBP); Figure S14 (<sup>1</sup>H NMR of P4VP(E-CNBP)<sub>0.5</sub>) (PDF)

## AUTHOR INFORMATION

### Corresponding Author

\*E-mail [xfchen75@suda.edu.cn](mailto:xfchen75@suda.edu.cn) (X.-F.C.).

### ORCID

Xiao-Fang Chen: 0000-0002-2973-0432

### Notes

The authors declare no competing financial interest.

## ACKNOWLEDGMENTS

This work was supported by the National Natural Science Foundation of China (Grants 21474073 and 21174003) and A Priority Academic Program Development of Jiangsu Higher Education Institutions (PAPD) for financial support. We thank Beamline BL16B1 at SSRF (Shanghai Synchrotron Radiation Facility, China) for providing the beamtimes.

## REFERENCES

(1) Herbert, K. M.; Schrettl, S.; Rowan, S. J.; Weder, C. 50th anniversary perspective: Solid-state multistimuli, multiresponsive polymeric materials. *Macromolecules* **2017**, *50*, 8845–8870.

- (2) Ercole, F.; Davis, T. P.; Evans, R. A. Photo-responsive systems and biomaterials: Photochromic polymers, light-triggered self-assembly, surface modification, fluorescence modulation and beyond. *Polym. Chem.* **2010**, *1*, 37–54.
- (3) Kim, H. N.; Guo, Z. Q.; Zhu, W. H.; Yoon, J.; Tian, H. Recent progress on polymer-based fluorescent and colorimetric chemosensors. *Chem. Soc. Rev.* **2011**, *40*, 79–93.
- (4) Zhang, J. J.; Zou, Q.; Tian, H. Photochromic materials: More than meets the eye. *Adv. Mater.* **2013**, *25*, 378–399.
- (5) Yao, X. Y.; Li, T.; Wang, J.; Ma, X.; Tian, H. Recent progress in photoswitchable supramolecular self-assembling systems. *Adv. Opt. Mater.* **2016**, *4*, 1322–1349.
- (6) Wei, P.; Zhang, J. X.; Zhao, Z.; Chen, Y. C.; He, X. W.; Chen, M.; Gong, J. Y.; Sung, H. H. Y.; Williams, I. D.; Lam, J. W. Y.; Tang, B. Z. Multiple yet controllable photoswitching in a single AIEgen system. *J. Am. Chem. Soc.* **2018**, *140*, 1966–1975.
- (7) An, B. K.; Kwon, S. K.; Jung, S. D.; Park, S. Y. Enhanced emission and its switching in fluorescent organic nanoparticles. *J. Am. Chem. Soc.* **2002**, *124*, 14410–14415.
- (8) An, B. K.; Kwon, S. K.; Park, S. Y. Photopatterned arrays of fluorescent organic nanoparticles. *Angew. Chem., Int. Ed.* **2007**, *46*, 1978–1982.
- (9) Zhu, L. L.; Ang, C. Y.; Li, X.; Nguyen, K. T.; Tan, S. Y.; Agren, H.; Zhao, Y. L. Luminescent color conversion on cyanostilbene-functionalized quantum dots via in-situ photo-tuning. *Adv. Mater.* **2012**, *24*, 4020–4024.
- (10) An, B. K.; Gierschner, J.; Park, S. Y. pi-Conjugated cyanostilbene derivatives: A unique self-assembly motif for molecular nanostructures with enhanced emission and transport. *Acc. Chem. Res.* **2012**, *45*, 544–554.
- (11) Zhu, L. L.; Zhao, Y. L. Cyanostilbene-based intelligent organic optoelectronic materials. *J. Mater. Chem. C* **2013**, *1*, 1059–1065.
- (12) Hong, Y.; Lam, J. W. Y.; Tang, B. Z. Aggregation-induced emission: Phenomenon, mechanism and applications. *Chem. Commun.* **2009**, 4332–4353.
- (13) Hong, Y.; Lam, J. W. Y.; Tang, B. Z. Aggregation-induced emission. *Chem. Soc. Rev.* **2011**, *40*, 5361–5388.
- (14) Mei, J.; Leung, N. L. C.; Kwok, R. T. K.; Lam, J. W. Y.; Tang, B. Z. Aggregation-induced emission: Together we shine, united we soar! *Chem. Rev.* **2015**, *115*, 11718–11940.
- (15) Yoon, S. J.; Chung, J. W.; Gierschner, J.; Kim, K. S.; Choi, M. G.; Kim, D.; Park, Y. S. Multistimuli two-color luminescence switching via different slip-stacking of highly fluorescent molecular sheets. *J. Am. Chem. Soc.* **2010**, *132*, 13675–13683.
- (16) Dou, C.; Han, L.; Zhao, S.; Zhang, H.; Wang, Y. Multi-stimuli-responsive fluorescence switching of a donor–acceptor  $\pi$ -conjugated compound. *J. Phys. Chem. Lett.* **2011**, *2*, 666–670.
- (17) Zhang, Y. J.; Sun, J. W.; Bian, G. F.; Chen, Y. Y.; Ouyang, M.; Hu, B.; Zhang, C. Cyanostilben-based derivatives: Mechanical stimuli-responsive luminophors with aggregation-induced emission enhancement. *Photochem. Photobiol. Sci.* **2012**, *11*, 1414–1421.
- (18) Yoon, S.-J.; Park, S. Polymorphic and mechanochromic luminescence modulation in the highly emissive dicyanodistyrylbenzene crystal: Secondary bonding interaction in molecular stacking assembly. *J. Mater. Chem.* **2011**, *21*, 8338–8336.
- (19) Zhang, Y.; Sun, J.; Lv, X.; Ouyang, M.; Cao, F.; Pan, G.; Pan, L.; Fan, G.; Yu, W.; He, C.; Zheng, S.; Zhang, F.; Wang, W.; Zhang, C. Heating and mechanical force-induced “turn on” fluorescence of cyanostilbene derivative with H-type stacking. *CrystEngComm* **2013**, *15*, 8998–9002.
- (20) Zhang, Y. J.; Zhuang, G. L.; Ouyang, M.; Hu, B.; Song, Q. B.; Sun, J. W.; Zhang, C.; Gu, C.; Xu, Y. X.; Ma, Y. G. Mechanochromic and thermochromic fluorescent properties of cyanostilbene derivatives. *Dyes Pigm.* **2013**, *98*, 486–492.
- (21) Zhang, Y. Y.; Li, H. F.; Zhang, G. B.; Xu, X. Y.; Kong, L.; Tao, X. T.; Tian, Y. P.; Yang, J. X. Aggregation-induced emission enhancement and mechanofluorochromic properties of alpha-cyanostilbene functionalized tetraphenyl imidazole derivatives. *J. Mater. Chem. C* **2016**, *4*, 2971–2978.
- (22) Zhao, H.; Wang, Y. T.; Harrington, S.; Ma, L.; Hu, S. Z.; Wu, X.; Tang, H.; Xue, M.; Wang, Y. B. Remarkable substitution influence on the mechanochromism of cyanostilbene derivatives. *RSC Adv.* **2016**, *6*, 66477–66483.
- (23) Yoon, S. J.; Kim, J. H.; Kim, K. S.; Chung, J. W.; Heinrich, B.; Mathevet, F.; Kim, P.; Donnio, B.; Attias, A. J.; Kim, D.; Park, S. Y. Mesomorphic organization and thermochromic luminescence of dicyanodistyrylbenzene-based phasmidic molecular disks: Uniaxially aligned hexagonal columnar liquid crystals at room temperature with enhanced fluorescence emission and semiconductivity. *Adv. Funct. Mater.* **2012**, *22*, 61–69.
- (24) Kim, H.; Chang, J. Y. Reversible thermochromic polymer film embedded with fluorescent organogel nanofibers. *Langmuir* **2014**, *30*, 13673–13679.
- (25) Martinez-Abadia, M.; Varghese, S.; Milian-Medina, B.; Gierschner, J.; Gimenez, R.; Ros, M. B. Bent-core liquid crystalline cyanostilbenes: Fluorescence switching and thermochromism. *Phys. Chem. Chem. Phys.* **2015**, *17*, 11715–11724.
- (26) Palakollu, V.; Kanvah, S.  $\alpha$ -Cyanostilbene based fluorophores: Aggregation-induced enhanced emission, solvatochromism and the pH effect. *New J. Chem.* **2014**, *38*, 5736–5746.
- (27) Park, S. K.; Cho, I.; Gierschner, J.; Kim, J. H.; Kim, J. H.; Kwon, J. E.; Kwon, O. K.; Whang, D. R.; Park, J. H.; An, B. K.; Park, S. Y. Stimuli-responsive reversible fluorescence switching in a crystalline donor-acceptor mixture film: Mixed stack charge-transfer emission versus segregated stack monomer emission. *Angew. Chem., Int. Ed.* **2016**, *55*, 203–207.
- (28) Gulino, A.; Lupo, F.; Condorelli, G. G.; Fragala, M. E.; Amato, M. E.; Scarlata, G. Reversible photoswitching of stimuli-responsive Si(100) surfaces engineered with an assembled 1-cyano-1-phenyl-2-(4'-(10-undecenyloxy)phenyl-ethylene monolayer. *J. Mater. Chem.* **2008**, *18* (41), 5011–5018.
- (29) Chung, J. W.; Yoon, S. J.; An, B. K.; Park, S. Y. High-contrast on/off fluorescence switching via reversible E–Z isomerization of diphenylstilbene containing the  $\alpha$ -cyanostilbenic moiety. *J. Phys. Chem. C* **2013**, *117*, 11285–11291.
- (30) Zhu, L. L.; Li, X.; Zhang, Q.; Ma, X.; Li, M. H.; Zhang, H. C.; Luo, Z.; Agren, H.; Zhao, Y. L. Unimolecular photoconversion of multicolor luminescence on hierarchical self-assemblies. *J. Am. Chem. Soc.* **2013**, *135*, 5175–5182.
- (31) Seo, J.; Chung, J. W.; Kwon, J. E.; Park, S. Y. Photoisomerization-induced gel-to-sol transition and concomitant fluorescence switching in a transparent supramolecular gel of a cyanostilbene derivative. *Chem. Sci.* **2014**, *5*, 4845–4850.
- (32) Lu, H. B.; Qiu, L. Z.; Zhang, G. Y.; Ding, A. X.; Xu, W. B.; Zhang, G. B.; Wang, X.; Kong, L.; Tian, Y. P.; Yang, J. X. Electrically switchable photoluminescence of fluorescent-molecule-dispersed liquid crystals prepared via photoisomerization-induced phase separation. *J. Mater. Chem. C* **2014**, *2*, 1386–1389.
- (33) Park, J. W.; Nagano, S.; Yoon, S. J.; Dohi, T.; Seo, J.; Seki, T.; Park, S. Y. High contrast fluorescence patterning in cyanostilbene-based crystalline thin films: Crystallization-induced mass flow via a photo-triggered phase transition. *Adv. Mater.* **2014**, *26*, 1354–1359.
- (34) Xing, P. Y.; Chen, H. Z.; Bai, L. Y.; Zhao, Y. L. Photo-triggered transformation from vesicles to branched nanotubes fabricated by a cholesterol-appended cyanostilbene. *Chem. Commun.* **2015**, *51*, 9309–9312.
- (35) Jin, Y.; Xia, Y.; Wang, S.; Yan, L.; Zhou, Y.; Fan, J.; Song, B. Concentration-dependent and light-responsive self-assembly of bolaamphiphiles bearing alpha-cyanostilbene based photochromophore. *Soft Matter* **2015**, *11*, 798–805.
- (36) Gao, R.; Cao, D.; Guan, Y.; Yan, D. Flexible self-supporting nanofibers thin films showing reversible photochromic fluorescence. *ACS Appl. Mater. Interfaces* **2015**, *7*, 9904–9910.
- (37) Lu, H. B.; Wu, S. J.; Zhang, C. L.; Qiu, Z.; Wang, X. H.; Zhang, G. B.; Hu, J. T.; Yang, J. X. Photoluminescence intensity and polarization modulation of a light emitting liquid crystal via reversible isomerization of an alpha-cyanostilbenic derivative. *Dyes Pigm.* **2016**, *128*, 289–295.

- (38) Yang, M. M.; Xing, P. Y.; Ma, M. F.; Zhang, Y. M.; Wang, Y. J.; Hao, A. Y. Controlled self-organization of cyanostilbene: Emission tuning and photo-responsiveness. *Soft Matter* **2016**, *12*, 6038–6042.
- (39) Martinez-Abadia, M.; Robles-Hernandez, B.; de la Fuente, M. R.; Gimenez, R.; Ros, M. B. Photoresponsive cyanostilbene bent-core liquid crystals as new materials with light-driven modulated polarization. *Adv. Mater.* **2016**, *28*, 6586–6591.
- (40) Li, J.; Zhang, Z.; Tian, J.; Li, G.; Wei, J.; Guo, J. Dicyanodistyrylbenzene-based chiral fluorescence photoswitches: An emerging class of multifunctional switches for dual-mode phototunable liquid crystals. *Adv. Opt. Mater.* **2017**, *5*, 1700014.
- (41) Ruokolainen, J.; tenBrinke, G.; Ikkala, O.; Torkkeli, M.; Serimaa, R. Mesomorphic structures in flexible polymer surfactant systems due to hydrogen bonding: Poly(4-vinylpyridine)-pentadecylphenol. *Macromolecules* **1996**, *29* (10), 3409–3415.
- (42) Ruokolainen, J.; ten Brinke, G.; Ikkala, O. Supramolecular polymeric materials with hierarchical structure-within-structure morphologies. *Adv. Mater.* **1999**, *11*, 777–780.
- (43) Ikkala, O.; ten Brinke, G. Functional materials based on self-assembly of polymeric supramolecules. *Science* **2002**, *295*, 2407–2409.
- (44) Hammond, M. R.; Mezzenga, R. Supramolecular routes towards liquid crystalline side-chain polymers. *Soft Matter* **2008**, *4*, 952–961.
- (45) Rosen, B. M.; Wilson, C. J.; Wilson, D. A.; Peterca, M.; Imam, M. R.; Percec, V. Dendron-mediated self-assembly, disassembly, and self-organization of complex systems. *Chem. Rev.* **2009**, *109*, 6275–6540.
- (46) Kao, J.; Thorkelsson, K.; Bai, P.; Rancatore, B. J.; Xu, T. Toward functional nanocomposites: Taking the best of nanoparticles, polymers, and small molecules. *Chem. Soc. Rev.* **2013**, *42*, 2654–2678.
- (47) Maggini, L.; Bonifazi, D. Hierarchised luminescent organic architectures: Design, synthesis, self-assembly, self-organisation and functions. *Chem. Soc. Rev.* **2012**, *41*, 211–241.
- (48) Zhu, X. M.; Beginn, U.; Möller, M.; Gearba, R. I.; Anokhin, D. V.; Ivanov, D. A. Self-organization of polybases neutralized with mesogenic wedge-shaped sulfonic acid molecules: An approach toward supramolecular cylinders. *J. Am. Chem. Soc.* **2006**, *128*, 16928–16937.
- (49) Tennesi, K. K.; Chen, X. F.; Li, C. Y.; Wan, X. H.; Fan, X. H.; Zhou, Q. F.; Rong, L. X.; Hsiao, B. S. Hierarchical nanostructures of bent-core molecules blended with poly(styrene-*b*-4-vinylpyridine) block copolymer. *Macromolecules* **2007**, *40*, 5095–5102.
- (50) Cheng, Z. Y.; Ren, B. Y.; Shan, H. Z.; Liu, X. X.; Tong, Z. Mesomorphous structure change induced by binding site difference in ionic complexes of linear polymers and dendritic amphiphiles. *Macromolecules* **2008**, *41*, 2656–2662.
- (51) Chuang, W. T.; Sheu, H. S.; Jeng, U. S.; Wu, H. H.; Hong, P. D.; Lee, J. J. Tetragonally perforated layer structure via columnar ordering of 4'-(3,4,5-trioctyloxybenzoyloxy)benzoic acid in a supramolecular complex with polystyrene-*block*-poly(4-vinylpyridine). *Chem. Mater.* **2009**, *21*, 975–978.
- (52) Wang, S. J.; Xu, Y. S.; Yang, S.; Chen, E. Q. Phase behavior of a hydrogen-bonded polymer with lamella-to-cylinder transition: Complex of poly(4-vinylpyridine) and small dendritic benzoic acid derivative. *Macromolecules* **2012**, *45*, 8760–8769.
- (53) Liu, X. S.; Chen, X. F.; Wang, J. K.; Chen, G.; Zhang, H. L. Hydrogen-bonded polymers with bent-shaped side chains and poly(4-vinylpyridine) backbone: Phase behavior and thin film morphologies. *Macromolecules* **2014**, *47*, 3917–3925.
- (54) Wang, S. J.; Zhao, R. Y.; Yang, S.; Yu, Z. Q.; Chen, E. Q. A complex of poly(4-vinylpyridine) and toluene based hemi-phasmid benzoic acid: Towards luminescent supramolecular side-chain liquid crystalline polymers. *Chem. Commun.* **2014**, *50*, 8378–8381.
- (55) Yan, J. T.; Li, W.; Zhang, A. Dendronized supramolecular polymers. *Chem. Commun.* **2014**, *50*, 12221–12233.
- (56) Wang, J. K.; Ma, S. H.; Chen, X. F.; Chen, H. Hydrogen-bonded liquid crystalline polymers containing poly(4-vinylpyridine) and dendron-like side chains: From lamellar to columnar phase. *Mater. Today Commun.* **2015**, *4*, 77–85.
- (57) Cai, Y.; Zheng, M.; Zhu, Y.; Chen, X. F.; Li, C. Y. Tunable supramolecular hexagonal columnar structures of hydrogen-bonded copolymers containing two different sized dendritic side chains. *ACS Macro Lett.* **2017**, *6*, 479–484.
- (58) Zheng, M. Q.; Zhu, Y. L.; Chen, X. F.; Li, C. Y. Mesomorphic phase behaviour of hydrogen-bonded supramolecular copolymers containing dendritic and linear side chains. *Acta Polym. Sin.* **2017**, *10*, 1624–1632.
- (59) Peng, H. Q.; Zheng, X. Y.; Han, T.; Kwok, R. T. K.; Lam, J. W. Y.; Huang, X. H.; Tang, B. Z. Dramatic differences in aggregation-induced emission and supramolecular polymerizability of tetraphenylethene-based stereoisomers. *J. Am. Chem. Soc.* **2017**, *139*, 10150–10156.
- (60) Chung, J. W.; You, Y.; Huh, H. S.; An, B. K.; Yoon, S. J.; Kim, S. H.; Lee, S. W.; Park, S. Y. Shear- and UV-induced fluorescence switching in stilbenic pi-dimer crystals powered by reversible [2 + 2] cycloaddition. *J. Am. Chem. Soc.* **2009**, *131*, 8163–8172.
- (61) Martinez-Abadia, M.; Varghese, S.; Gimenez, R.; Ros, M. B. Multiresponsive luminescent dicyanodistyrylbenzenes and their photochemistry in solution and in bulk. *J. Mater. Chem. C* **2016**, *4*, 2886–2893.
- (62) Martinez-Abadia, M.; Varghese, S.; Romero, P.; Gierschner, J.; Gimenez, R.; Ros, M. B. Highly light-sensitive luminescent cyanostilbene flexible dimers. *Adv. Opt. Mater.* **2017**, *5*, 1600860.